Shining Light on Transition-Metal Oxides: Unveiling the Hidden Fermi Liquid

Xiaoyu Deng,[1] Aaron Sternbach,[2] Kristjan Haule,[1] D. N. Basov,[2] and Gabriel Kotliar[1]
[1]Department of Physics and Astronomy, Rutgers University, Piscataway, New Jersey 08854, USA
[2]Department of Physics, University of California San Diego, La Jolla, California 92093, USA
(Received 25 April 2014; published 8 December 2014)

We use low energy optical spectroscopy and first principles local density approximation plus dynamical mean field theory calculations to test the hypothesis that the anomalous transport properties of strongly correlated metals originate in the strong temperature dependence of their underlying resilient quasiparticles. We express the resistivity in terms of an effective plasma frequency ω_p^* and an effective scattering rate $1/\tau_{\rm tr}^*$. We show that in the archetypal correlated material V_2O_3, ω_p^* increases with increasing temperature, while the plasma frequency from the partial sum rule exhibits the opposite trend. $1/\tau_{\rm tr}^*$ has a more pronounced temperature dependence than the scattering rate obtained from the extended Drude analysis. The theoretical calculations of these quantities are in quantitative agreement with experiment. We conjecture that these are robust properties of all strongly correlated metals, and test the conjecture by carrying out a similar analysis on thin film $NdNiO_3$ on a $LaAlO_3$ substrate.

DOI: 10.1103/PhysRevLett.113.246404 PACS numbers: 71.27.+a, 72.10.-d, 78.20.-e

Understanding the transport properties in metallic states of strongly correlated materials is a long-standing challenge in condensed matter physics. Many correlated metals are not canonical Landau Fermi liquids (LFLs) as their resistivities do not follow the T^2 law in a broad temperature range. Fermi liquid behavior emerges only below a very low temperature scale $T_{\rm LFL}$, which can be vanishingly small or hidden by the onset of some form of long range order. Above $T_{\rm LFL}$, the resistivity usually rises smoothly and eventually exceeds the Mott-Ioffe-Regel limit, entering the so-called "bad metal" regime [1] with no clear sign of saturation [2,3]. As stressed in Ref. [1] an interpretation of the transport properties in terms of quasiparticles (QPs) is problematic when the mean free path is comparable with the de Broglie wavelength of the carriers, and describing the charge transport above $T_{\rm LFL}$ is an important challenge for the theory of strongly correlated materials.

It was shown in the context of the interacting electron-phonon system, that the QP picture is actually valid in regimes that fall outside the LFL hypothesis [4]. There are peaks in the spectral functions that define renormalized QPs even though the QP scattering rate is comparable to the QP energy. The transport properties can be formulated in terms of a transport Boltzman kinetic equation for the QP distribution function, which has precisely the form proposed by Landau [5,6]. Solving the transport equation, the dc conductivity can be expressed as

$$\sigma_{\rm dc} = (\omega_p^*)^2 \tau_{\rm tr}^*/4\pi \qquad (1)$$

in analogy with the Drude formula. The effective transport scattering rate $1/\tau_{\rm tr}^*$ characterizes the decay of QPs due to collisions involving Umklapp process, and ω_p^* is the low energy effective plasma frequency.

The temperature dependence of the transport coefficients beyond the scope of LFL and many salient features seen in correlated oxides, such as their low coherence scale, nonsaturating resistivities, and anomalous transfer of spectral weight, are described well in studies of the doped Hubbard model within the framework of dynamical field mean theory (DMFT) (for early reviews of this topic see Refs. [7,8]). A complete understanding of the transport anomalies has been reached recently [9–11]. As in the Prange-Kadanoff theory [4], the QPs are resilient, surviving in a broad region above $T_{\rm LFL}$ [10], and a quantum kinetic equation provides a quantitative description of the transport [11].

While in the electron-phonon coupled system treated in Ref. [4] the Fermi liquid parameters such as the QP velocities and therefore ω_p^* are temperature independent, they are strongly temperature dependent in the doped Mott insulator within DMFT due to changes in the Fermi surface at high temperatures [9,10] and a strong temperature dependence of the effective mass at intermediate temperatures [10,11]. This strong temperature dependence of ω_p^* hides the more conventional temperature dependence of $1/\tau_{\rm tr}^*$ in the resistivity, which is quadratic in a broad region of temperatures and has saturating behavior at high temperatures [11]. The strong temperature dependence in the QP electronic structure with the resulting temperature dependence of ω_p^* and $1/\tau_{\rm tr}^*$ thus provides a simple scenario to describe the anomalous transport of correlated metals.

In this Letter, we provide experimental and theoretical evidence that this picture holds beyond the DMFT treatment of the simplified Hubbard model, and is indeed relevant to real materials. We focus on V_2O_3. This archetypal correlated material provided the first experimental corroboration of the validity of the DMFT picture of

the Mott transition [12] and is still a subject of intense experimental studies [13–17]. We extract the effective plasma frequency ω_p^* and effective scattering rate $1/\tau_{\rm tr}^*$ from the optical conductivity as described below and show that they display the predicted temperature dependence. We contrast their temperature dependence to that of the plasma frequency and scattering rate extracted from the standard extended Drude analysis.

In correlated systems the optical conductivity is usually parametrized with the so-called extended Drude analysis in terms of two frequency dependent quantities, the scattering rate $1/\tau(\omega)$ and the mass enhancement $m^*(\omega)/m_b$ [18],

$$\sigma(\omega) = \sigma_1(\omega) + i\sigma_2(\omega) = \frac{\omega_p^2}{4\pi}\frac{1}{-i\omega\frac{m^*(\omega)}{m_b} + 1/\tau(\omega)}. \quad (2)$$

The plasma frequency ω_p is obtained with the partial sum rule $(\omega_p^2/8) = \int_0^\Omega \sigma_1(\omega)d\omega$ and depends on the cutoff Ω chosen so as to exclude interband transitions. To test the theory, instead we focus on quantities that have a simple QP interpretation, namely $1/\tau_{\rm tr}^*$ and $(\omega_p^*)^2$, from the low frequency optical conductivity extracted as follows:

$$(\omega_p^*)^2 = 4\pi\frac{\sigma_1^2+\sigma_2^2}{\sigma_2/\omega}\bigg|_{\omega\to 0}, \qquad 1/\tau_{\rm tr}^* = \frac{\sigma_1}{\sigma_2/\omega}\bigg|_{\omega\to 0}. \quad (3)$$

When a direct determination of the imaginary part of the optical conductivity (as for example in ellipsometry measurements) is not available, they can be extracted from $\sigma_1(\omega)$ only, using

$$\frac{\sigma_2(\omega)}{\omega}\bigg|_{\omega\to 0} = -\frac{1}{\pi}\int_{-\infty}^{\infty}\frac{1}{\omega'}\frac{\partial\sigma_1(\omega')}{\partial\omega'}d\omega'. \quad (4)$$

Comparing with the extended Drude analysis, we have $(\omega_p^*)^2 = (m_b/m^*(0))\omega_p^2$, $(1/\tau_{\rm tr}^*) = (m_b/m^*(0))(1/\tau(0))$. Thus, this analysis is related to the extended Drude analysis, but is free of the partial sum rule. Similar low frequency analysis has been used in previous works [18–24]; however, the temperature dependence of ω_p^* and $(1/\tau_{\rm tr}^*)$ was not the focus of those studies.

We apply the proposed analysis to V_2O_3, a prototypical material exhibiting a metal insulator transition (MIT) [25,26]. Pure V_2O_3 is a paramagnetic metal (PM) at ambient conditions. It enters the antiferromagnetic insulating state (AFI) below $T_N \simeq 150$ K with a concomitant structural transition, and the AFI can be quenched by Ti doping or pressure. The PM can be turned into a paramagnetic insulator by slight Cr doping, which induces a first order isostructural transition with a small change in the c/a ratio, indicating a typical band-controlled MIT scenario [27]. This first order transition ends at a second order critical point at a temperature around 400 K [13,26]. The PM phase exhibits significant signatures of correlations; for instance, a pronounced QP peak and a broad lower Hubbard band were revealed in photoemission spectroscopy measurements [28–30]. The PM phase is a Fermi liquid at low temperature when the AFI is suppressed [31].

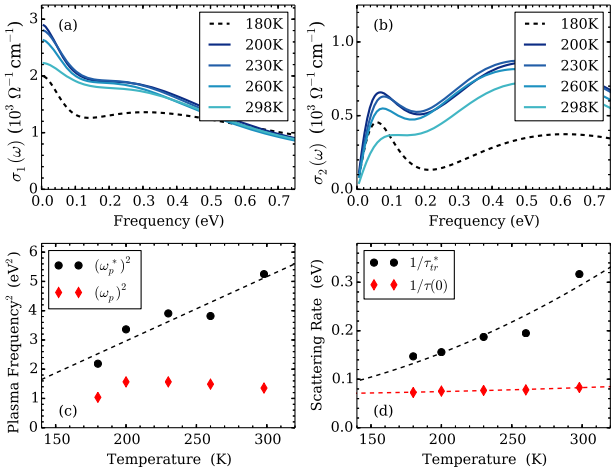

FIG. 1 (color online). Optical conductivity (a) $\sigma_1(\omega)$ and (b) $\sigma_2(\omega)$ of V_2O_3 at different temperatures is taken from Ref. [16], where dashed lines indicate data at $T = 180$ K very close to the MIT. (c) $(\omega_p^*)^2$ and (d) $1/\tau_{\rm tr}^*$ of V_2O_3 are extracted according to Eq. (3). ω_p^2 and $1/\tau(0)$ extracted from the extended Drude analysis are shown for comparison. Dashed lines are guides for the eye by fitting $(\omega_p^*)^2$ and $1/\tau_{\rm tr}^*$ $[1/\tau(0)]$ to linear $(a+bT)$ and parabolic $(c+dT^2)$ functions, respectively.

Figures 1(a) and 1(b) show the measured optical conductivity $\sigma(\omega) = \sigma_1(\omega) + i\sigma_2(\omega)$ of pure V_2O_3 in the PM phase [16]. Pronounced Drude peaks show up even when the resistivity is high (of the order of 1 $m\Omega^{-1}\,cm^{-1}$) and does not follow the T^2 law [13,32]. The Drude peak diminishes gradually upon increasing temperature, except at the lowest temperature where the transport is probably affected by the precursor of the ordered phase. ω_p^* and $1/\tau_{\rm tr}^*$ extracted according to Eq. (3) are shown in Figs. 1(c) and 1(d). We find that $(\omega_p^*)^2$ increases with increasing temperature. This is in contrast with $(\omega_p)^2$ obtained by the partial sum rule with a cutoff $\Omega = 140$ meV, which slightly decreases [16] except at the lowest temperature where precursors to the ordered phase such as magnetism and electronic heterogeneity tend to open a gap and reduce $(\omega_p)^2$. $1/\tau_{\rm tr}^*$ increases with increasing temperature and has the same trend as the scattering rate extracted with the extended Drude analysis at zero frequency $1/\tau(0)$, but with a much stronger temperature dependence. The experimental data are consistent with an $(\omega_p^*)^2$ that has a term linear and a $1/\tau_{\rm tr}^*$ that is quadratic in temperature, revealing a Fermi liquid behavior that is hidden in $1/\tau_{\rm tr}^*$. The analysis of the experimental data thus corroborates the main qualitative predictions of the DMFT description of transport properties in the simple model Hamiltonian [11].

We now argue that realistic local density approximation plus dynamical mean field theory (LDA+DMFT) [33,34] calculations describe well the optical properties as well as the extracted quantities ω_p^* and $1/\tau_{\rm tr}^*$; hence, a local

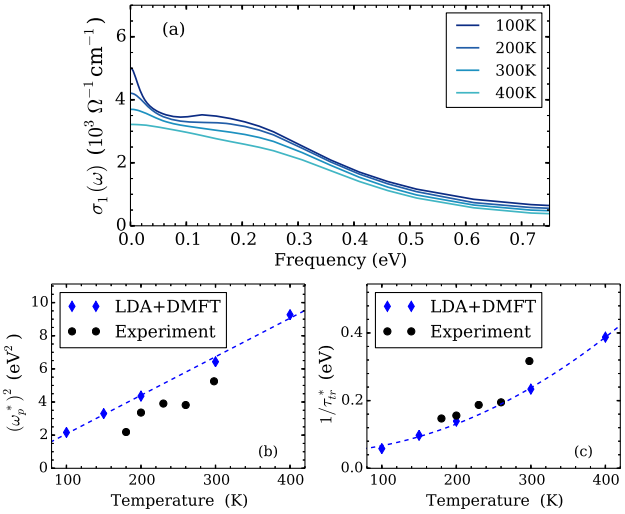

FIG. 2 (color online). (a) Optical conductivity of V_2O_3 calculated with the LDA+DMFT method. The effective plasma frequency (b) and effective scattering rate (c) are extracted using Eqs. (3) and (4) and compared to those extracted from experimental data. Dashed lines are guides to the eye by fitting $(\omega_p^*)^2$ and $1/\tau_{\mathrm{tr}}^*$ to linear $(a+bT)$ and parabolic $(c+dT^2)$ functions, respectively.

approximation, which ignores vertex corrections, is sufficiently accurate to capture the experimental trends. LDA+DMFT investigations on V_2O_3 by several groups have successfully described the properties of this material near the MIT [35–40]. The correlation in V_2O_3 is due to the partially filled narrow d orbitals with a nominal occupancy $n_d = 2$. The two electrons mainly populate the e_g^π and a_{1g} states of vanadium due to the surrounding oxygen octahedron with trigonal distortion. We perform the LDA+DMFT calculations and focus on the paramagnetic metallic phase only [41]. We treat e_g^π and a_{1g} orbitals dynamically with DMFT, and set the Coulomb interaction U and the Hund's coupling J to 6.0 and 0.8 eV, respectively. These parameters place V_2O_3 on the metallic side but close to the MIT. Various properties of V_2O_3 from our calculations are in good agreement with experimental results. For example, the calculated total spectra is consistent with experiment photoemission spectroscopy measurements [28–30]. The occupancies of the e_g^π and a_{1g} orbitals at $T = 200$ K are 1.60 and 0.50, respectively, in good agreement with x-ray absorption spectroscopy measurements [51].

We calculate the optical conductivity with the formalism presented in Ref. [52] in a broad temperature range as shown in Fig. 2(a). The main features of the experimental optical conductivity, the Drude peak and the shoulder structure at about 0.1 eV as well as their scale, are reasonably reproduced in our calculations. The Drude peak is gradually diminished and merges with the shoulder structure at around 400 K, in agreement with experiments [53]. Therefore, the LDA+DMFT calculation provides a satisfactory description of the optical properties of V_2O_3, except for the lowest temperature $T = 180$ K where effects such as short range order and heterogeneity in the proximity to the magnetic transition are not captured in our calculation. From the optical conductivity $(\omega_p^*)^2$ and $1/\tau_{\mathrm{tr}}^*$ are extracted using Eqs. (3) and (4). As shown in Figs. 2(b) and 2(c), they agree reasonably well with those extracted from experimental data. In particular, the same trends found with the experimental data, and thus the main characteristics of the "hidden" Fermi liquid behavior, show up more clearly in the broad temperature range studied in our calculations: $(\omega_p^*)^2$ appears linear and a $1/\tau_{\mathrm{tr}}^*$ appears quadratic versus temperature. Therefore, the proposed analysis of both the experimental data and the first principles calculations reveals a significant temperature dependence of the QPs in terms of $(\omega_p^*)^2$ and an extended quadratic temperature dependence of $1/\tau_{\mathrm{tr}}^*$, but not of $1/\tau(0)$.

To further understand these observations, let us recall the QP interpretation of the low frequency optical conductivity in the DMFT treatment of the doped single band Hubbard model. In this case, $\sigma(\omega)|_{\omega\to 0} = 2(m/m^*)\Phi^{xx}(\bar{\mu}) \times 1/(-i\omega + 2/\tau_{\mathrm{qp}}^*)$, in which m^*/m and τ_{qp}^* are the effective mass enhancement and the lifetime of the QPs, Φ is the transport function $\Phi^{xx}(\epsilon) = \sum_{\mathbf{k}}(\partial\epsilon_{\mathbf{k}}/\partial\mathbf{k}_x)^2\delta(\epsilon-\epsilon_{\mathbf{k}})$, and $\bar{\mu}$ is the effective chemical potential of the QPs [11]. Applying the analysis in Eq. (3), $(\omega_p^*)^2 = 8\pi(m/m^*) \times \Phi^{xx}(\bar{\mu})$ and $1/\tau_{\mathrm{tr}}^* = 2/\tau_{\mathrm{qp}}^*$. In the infinite dimension limit where DMFT is exact, the inverse of the effective mass enhancement m/m^* is numerically equal to the QP weight defined by $Z = (1 - (\partial \mathrm{Re}\Sigma(\omega)/\partial\omega))^{-1}$, where $\Sigma(\omega)$ is the self-energy. We note that in general the effective mass enhancement m^*/m enters the low frequency optical conductivity while the QP weight Z does not [5,6]. We also note that the effective mass enhancement m^*/m does not enter the plasma frequency in the textbook example of an interacting Fermi gas due to the presence of Galilean invariance and thus the cancellation of the vertex correction and effective mass enhancement [5,6]. However, the vertex correction is weak in realistic materials (especially in a three-dimensional structure with a large coordination number), which are much closer to the infinite-dimensional limit than the Galilean invariant idealization without important Umklapp process [54]. This justifies the good agreement between our results and experiments. The neglect of the vertex correction in DMFT thus leaves the QP weight in the plasma frequency. In situations where $\Phi(\bar{\mu})$ varies little with temperature, the observations above imply a strong temperature dependence of Z_{qp} and $1/\tau_{\mathrm{qp}}^*$. We emphasize that although a strong dependence of the scattering rate is generally expected in a Fermi liquid, the temperature dependence of the QP weight is not, but it was observed in model studies [10,11].

We then extract from our calculated self-energies, the QP weight Z defined above, and the QP scattering rate defined as $2/\tau_{\mathrm{qp}}^* = -2Z\mathrm{Im}\Sigma(0)$, which now are orbital dependent. The QP weight and the QP scattering rate are shown in Figs. 3(a) and 3(b). There is orbital differentiation

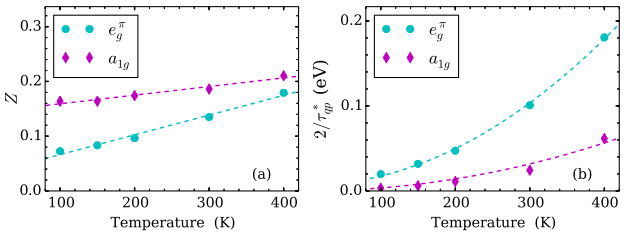

FIG. 3 (color online). The temperature dependence of the (a) QP weight $Z = (m/m^*) = (1 - (\partial \mathrm{Re}\Sigma(\omega)/\partial\omega))^{-1}$ and (b) effective scattering rate $2/\tau^*_{\mathrm{qp}} = -2Z\mathrm{Im}\Sigma(0)$ of V_2O_3 extracted from LDA+DMFT self-energies for e_g^π and a_{1g} orbitals. Dashed lines are guides for the eye by fitting Z and $2/\tau^*_{\mathrm{qp}}$ to linear $(a + bT)$ and parabolic $(c + dT^2)$ functions, respectively.

between the e_g^π and a_{1g} orbitals as pointed out in earlier studies [35,37]. Generally Z increases with increasing temperature and $1/\tau^*_{\mathrm{qp}}$ is approximately quadratic in temperature for both e_g^π and a_{1g} orbitals. The a_{1g} orbital is more coherent than the e_g^π orbital: $Z_{a_{1g}}$ is less temperature dependent and the effective QP scattering rate is smaller. It likely crosses over to the LFL regime below $T \simeq 150$ K where $Z_{a_{1g}}$ starts to saturate. Note that the e_g^π orbitals have a much larger spectral weight at the Fermi level than the a_{1g} orbital and thus dominate the transport. This pronounced temperature dependence is consistent with that of $(\omega_p^*)^2$ and $1/\tau^*_{\mathrm{tr}}$ extracted from the optical conductivity. Therefore, the properties of the underlying QPs, especially the temperature dependence of the QP weight and the QP scattering rate, are captured in our analysis on optical conductivities. We note that, in addition, the temperature dependence of the underlying QPs manifests itself in the temperature dependence of the effective chemical potentials of the QPs [41], which also contribute to the temperature dependence of $(\omega_p^*)^2$.

We expect that this picture of anomalous transport in correlated materials is not limited to V_2O_3 and is in fact generally applicable to various strongly correlated metals. To check the validity of this general conjecture we apply the same analysis to experimental data of a $NdNiO_3$ (NNO) film on a $LaAlO_3$ (LAO) substrate. NNO is another typical correlated material exhibiting a temperature-driven MIT [55]. While deposited as a film on a LAO substrate, the MIT can be quenched so that it remains metallic down to very low temperature [56]. High quality optical conductivities of a NNO film are taken from Ref [57] as shown in Figs. 4(a) and 4(b). We note that the resistivity is not T^2-like except possibly at the lowest temperature $T = 20$ K [56]. We perform the same analysis as above in V_2O_3. $(\omega_p^*)^2$ and $1/\tau^*_{\mathrm{tr}}$ are shown in Figs. 4(c) and 4(d) in comparison with ω_p^2 and $1/\tau(0)$ obtained by the extended Drude analysis with a cutoff of $\Omega = 125$ meV. Again we have the same features as in V_2O_3: $(\omega_p^*)^2$ increases almost linearly with increasing temperature and has the opposite trend with $(\omega_p)^2$, while $1/\tau^*_{\mathrm{tr}}$ has a more pronounced quadratic behavior in a wide temperature range well above T_{LFL}.

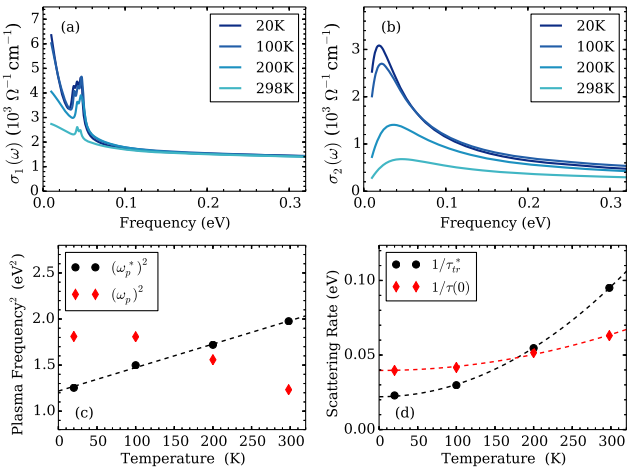

FIG. 4 (color online). Optical conductivity (a) $\sigma_1(\omega)$ and (b) $\sigma_2(\omega)$ of a NNO film on a LAO substrate at different temperatures is taken from Ref. [57], from which (c) $(\omega_p^*)^2$ and (d) $1/\tau^*_{\mathrm{tr}}$ are extracted according to Eq. (3). ω_p^2 and $1/\tau(0)$ extracted from the extended Drude analysis are shown for comparison. Dashed lines are guides for the eye by fitting $(\omega_p^*)^2$ and $1/\tau^*_{\mathrm{tr}}$ $[1/\tau(0)]$ to linear $(a + bT)$ and parabolic $(c + dT^2)$ functions, respectively.

In conclusion, in this Letter we point out and establish by analyzing both the experimental and the theoretical data that the anomalous transport properties observed in many transition-metal oxides arise from a temperature dependent $(\omega_p^*)^2$ and $1/\tau^*_{\mathrm{tr}}$. The quadratic dependence of the QP scattering rate hidden from the resistivity is not confined to Mott-Hubbard systems but occurs also in a Hund's metal such as $CaRuO_3$ [41]. Further investigations should be carried out in other compounds, starting from systems where there are already preliminary indications, such as nickelates, pnictides, and cuprates [58–60], with a temperature dependent $m^*(0)/m_b$ seen in the extended Drude analysis. Finally, high resolution studies using spectroscopies such as ARPES and STM in quasiparticle interference mode would be very useful to separate the various contributions to the temperature dependence of $(\omega_p^*)^2$ by probing directly the electronic structure.

We acknowledge very useful discussions with A. Georges and P. Armitage. This work was supported by NSF DMR-1308141 (X. D. and G. K), NSF DMR 1405303 (K. H.) and ARO w911NF-13-1-0210 (A. S. and D. N. B.). Computations were made possible using NSF EAGER DMR-1342921.

[1] V. J. Emery and S. A. Kivelson, Phys. Rev. Lett. **74**, 3253 (1995).
[2] N. Hussey, K. Takenaka, and H. Takagi, Philos. Mag. **84**, 2847 (2004).
[3] O. Gunnarsson, M. Calandra, and J. E. Han, Rev. Mod. Phys. **75**, 1085 (2003).

[4] R. E. Prange and L. P. Kadanoff, Phys. Rev. **134**, A566 (1964).

[5] D. Pines and P. Nozières, *Theory of Quantum Liquids: Normal Fermi Liquids* (Perseus Books, Cambridge, MA, 1999), Vol. I.

[6] P. Nozières, *Theory of Interacting Fermi Systems* (Addison-Wesley, Reading, MA, 1997).

[7] T. Pruschke, M. Jarrell, and J. Freericks, Adv. Phys. **44**, 187 (1995).

[8] A. Georges, G. Kotliar, W. Krauth, and M. J. Rozenberg, Rev. Mod. Phys. **68**, 13 (1996).

[9] G. Pálsson and G. Kotliar, Phys. Rev. Lett. **80**, 4775 (1998).

[10] X. Deng, J. Mravlje, R. Žitko, M. Ferrero, G. Kotliar, and A. Georges, Phys. Rev. Lett. **110**, 086401 (2013).

[11] W. Xu, K. Haule, and G. Kotliar, Phys. Rev. Lett. **111**, 036401 (2013).

[12] M. J. Rozenberg, G. Kotliar, H. Kajueter, G. A. Thomas, D. H. Rapkine, J. M. Honig, and P. Metcalf, Phys. Rev. Lett. **75**, 105 (1995).

[13] P. Limelette, A. Georges, D. Jrome, P. Wzietek, P. Metcalf, and J. M. Honig, Science **302**, 89 (2003).

[14] S. Lupi *et al.*, Nat. Commun. **1**, 105 (2010).

[15] F. Rodolakis, P. Hansmann, J.-P. Rueff, A. Toschi, M. W. Haverkort, G. Sangiovanni, A. Tanaka, T. Saha-Dasgupta, O. K. Andersen, K. Held, M. Sikora, I. Alliot, J.-P. Itié, F. Baudelet, P. Wzietek, P. Metcalf, and M. Marsi, Phys. Rev. Lett. **104**, 047401 (2010).

[16] M. K. Stewart, D. Brownstead, S. Wang, K. G. West, J. G. Ramirez, M. M. Qazilbash, N. B. Perkins, I. K. Schuller, and D. N. Basov, Phys. Rev. B **85**, 205113 (2012).

[17] Y. Ding, C.-C. Chen, Q. Zeng, H.-S. Kim, M. J. Han, M. Balasubramanian, R. Gordon, F. Li, L. Bai, D. Popov, S. M. Heald, T. Gog, H.-k. Mao, and M. van Veenendaal, Phys. Rev. Lett. **112**, 056401 (2014).

[18] D. N. Basov, R. D. Averitt, D. van der Marel, M. Dressel, and K. Haule, Rev. Mod. Phys. **83**, 471 (2011).

[19] W. Götze and P. Wölfle, Phys. Rev. B **6**, 1226 (1972).

[20] J. W. Allen and J. C. Mikkelsen, Phys. Rev. B **15**, 2952 (1977).

[21] S. Kamal, D. M. Kim, C. B. Eom, and J. S. Dodge, Phys. Rev. B **74**, 165115 (2006); S. Kamal, J. Dodge, D.-M. Kim, and C. B. Eom, in *Quantum Electronics and Laser Science Conference, 2005. QELS '05*, (IEEE , Baltimore, 2005) pp. 443–445.

[22] S. J. Youn, T. H. Rho, B. I. Min, and K. S. Kim, Phys. Status Solidi B **244**, 1354 (2007).

[23] A. Millis, in *Strong Interactions in Low Dimensions*, Physics and Chemistry of Materials with Low-Dimensional Structures Vol. 25 (Springer, Netherlands, 2004), pp. 195–235.

[24] N. P. Armitage, arXiv:0908.1126.

[25] D. B. McWhan, T. M. Rice, and J. P. Remeika, Phys. Rev. Lett. **23**, 1384 (1969).

[26] D. B. McWhan, A. Menth, J. P. Remeika, W. F. Brinkman, and T. M. Rice, Phys. Rev. B **7**, 1920 (1973).

[27] M. Imada, A. Fujimori, and Y. Tokura, Rev. Mod. Phys. **70**, 1039 (1998).

[28] S.-K. Mo, J. D. Denlinger, H.-D. Kim, J.-H. Park, J. W. Allen, A. Sekiyama, A. Yamasaki, K. Kadono, S. Suga, Y. Saitoh, T. Muro, P. Metcalf, G. Keller, K. Held, V. Eyert, V. I. Anisimov, and D. Vollhardt, Phys. Rev. Lett. **90**, 186403 (2003).

[29] F. Rodolakis, B. Mansart, E. Papalazarou, S. Gorovikov, P. Vilmercati, L. Petaccia, A. Goldoni, J. P. Rueff, S. Lupi, P. Metcalf, and M. Marsi, Phys. Rev. Lett. **102**, 066805 (2009).

[30] H. Fujiwara, A. Sekiyama, S.-K. Mo, J. W. Allen, J. Yamaguchi, G. Funabashi, S. Imada, P. Metcalf, A. Higashiya, M. Yabashi, K. Tamasaku, T. Ishikawa, and S. Suga, Phys. Rev. B **84**, 075117 (2011).

[31] D. B. McWhan, J. P. Remeika, J. P. Maita, H. Okinaka, K. Kosuge, and S. Kachi, Phys. Rev. B **7**, 326 (1973).

[32] D. B. McWhan, J. P. Remeika, T. M. Rice, W. F. Brinkman, J. P. Maita, and A. Menth, Phys. Rev. Lett. **27**, 941 (1971).

[33] G. Kotliar, S. Y. Savrasov, K. Haule, V. S. Oudovenko, O. Parcollet, and C. A. Marianetti, Rev. Mod. Phys. **78**, 865 (2006).

[34] K. Held, Adv. Phys. **56**, 829 (2007).

[35] K. Held, G. Keller, V. Eyert, D. Vollhardt, and V. I. Anisimov, Phys. Rev. Lett. **86**, 5345 (2001).

[36] M. S. Laad, L. Craco, and E. Müller-Hartmann, Phys. Rev. B **73**, 045109 (2006).

[37] A. I. Poteryaev, J. M. Tomczak, S. Biermann, A. Georges, A. I. Lichtenstein, A. N. Rubtsov, T. Saha-Dasgupta, and O. K. Andersen, Phys. Rev. B **76**, 085127 (2007).

[38] P. Hansmann, A. Toschi, G. Sangiovanni, T. Saha-Dasgupta, S. Lupi, M. Marsi, and K. Held, Phys. Status Solidi B **250**, 1251 (2013).

[39] D. Grieger, C. Piefke, O. E. Peil, and F. Lechermann, Phys. Rev. B **86**, 155121 (2012).

[40] J. M. Tomczak and S. Biermann, J. Phys. Condens. Matter **21**, 064209 (2009).

[41] See Supplementary Material at http://link.aps.org/supplemental/10.1103/PhysRevLett.113.246404, which includes Refs. [42–50], for the details of the LDA+DMFT calculations, the temperature dependence of the momentum-resolved spectra and QP bands of V_2O_3, and the hidden Fermi liquid behavior in $CaRuO_3$.

[42] P. Blaha, K. Schwarz, G. K. H. Madsen, D. Kvasnicka, and J. Luitz, *WIEN2 K, An Augmented Plane Wave + Local Orbitals Program for Calculating Crystal Properties* (Karlheinz Schwarz, Techn. Universität Wien, Austria, 2001).

[43] P. Werner, A. Comanac, L. de' Medici, M. Troyer, and A. J. Millis, Phys. Rev. Lett. **97**, 076405 (2006).

[44] K. Haule, Phys. Rev. B **75**, 155113 (2007).

[45] K. Inaba, A. Koga, S.-i. Suga, and N. Kawakami, Phys. Rev. B **72**, 085112 (2005).

[46] L. Klein, L. Antognazza, T. H. Geballe, M. R. Beasley, and A. Kapitulnik, Phys. Rev. B **60**, 1448 (1999).

[47] G. Cao, O. Korneta, S. Chikara, L. DeLong, and P. Schlottmann, Solid State Commun. **148**, 305 (2008).

[48] M. Schneider, D. Geiger, S. Esser, U. S. Pracht, C. Stingl, Y. Tokiwa, V. Moshnyaga, I. Sheikin, J. Mravlje, M. Scheffler, and P. Gegenwart, Phys. Rev. Lett. **112**, 206403 (2014).

[49] A. Georges, L. d. Medici, and J. Mravlje, Annu. Rev. Condens. Matter Phys. **4**, 137 (2013).

[50] Z. P. Yin, K. Haule, and G. Kotliar, Phys. Rev. B **86**, 195141 (2012).

[51] J.-H. Park, L. H. Tjeng, A. Tanaka, J. W. Allen, C. T. Chen, P. Metcalf, J. M. Honig, F. M. F. de Groot, and G. A. Sawatzky, Phys. Rev. B **61**, 11506 (2000).

[52] K. Haule, C.-H. Yee, and K. Kim, Phys. Rev. B **81**, 195107 (2010).
[53] L. Baldassarre, A. Perucchi, D. Nicoletti, A. Toschi, G. Sangiovanni, K. Held, M. Capone, M. Ortolani, L. Malavasi, M. Marsi, P. Metcalf, P. Postorino, and S. Lupi, Phys. Rev. B **77**, 113107 (2008).
[54] H. Maebashi and H. Fukuyama, J. Phys. Soc. Jpn. **67**, 242 (1998).
[55] J. B. Torrance, P. Lacorre, A. I. Nazzal, E. J. Ansaldo, and C. Niedermayer, Phys. Rev. B **45**, 8209 (1992).
[56] J. Liu, M. Kareev, B. Gray, J. W. Kim, P. Ryan, B. Dabrowski, J. W. Freeland, and J. Chakhalian, Appl. Phys. Lett. **96**, 233110 (2010).
[57] M. K. Stewart, J. Liu, M. Kareev, J. Chakhalian, and D. N. Basov, Phys. Rev. Lett. **107**, 176401 (2011).
[58] M. K. Stewart, C.-H. Yee, J. Liu, M. Kareev, R. K. Smith, B. C. Chapler, M. Varela, P. J. Ryan, K. Haule, J. Chakhalian, and D. N. Basov, Phys. Rev. B **83**, 075125 (2011).
[59] M. M. Qazilbash, J. J. Hamlin, R. E. Baumbach, L. Zhang, D. J. Singh, M. B. Maple, and D. N. Basov, Nat. Phys. **5**, 647 (2009).
[60] S. I. Mirzaei, D. Stricker, J. N. Hancock, C. Berthod, A. Georges, E. van Heumen, M. K. Chan, X. Zhao, Y. Li, M. Greven, N. Barii, and D. van der Marel, Proc. Natl. Acad. Sci. U.S.A. **110**, 5774 (2013).